PARTIAL CONTROL OF ESCAPES IN CHAOTIC SCATTERING

MATTIA COCCOLO

Nonlinear Dynamics, Chaos and Complex Systems Group,
Departamento de Física, Universidad Rey Juan Carlos,
Tulipán s/n, 28933 Móstoles, Madrid, Spain

JESÚS M. SEOANE

Nonlinear Dynamics, Chaos and Complex Systems Group,
Departamento de Física, Universidad Rey Juan Carlos,
Tulipán s/n, 28933 Móstoles, Madrid, Spain

SAMUEL ZAMBRANO

San Raffaele University, Via Olgettina 58, 20132 Milan, Italy

MIGUEL A. F. SANJUÁN

Nonlinear Dynamics, Chaos and Complex Systems Group,
Departamento de Física, Universidad Rey Juan Carlos,
Tulipán s/n, 28933 Móstoles, Madrid, Spain

Chaotic scattering in open Hamiltonian systems is relevant for different problems in physics. Particles in such kind of systems can exhibit both bounded or unbounded motions for which escapes from the scattering region can take place. This paper analyzes how to control the escape of the particles from the scattering region in the presence of noise. For that purpose, we apply the partial control technique to the Hénon–Heiles system, which implies that we need to use a control smaller than the noise present in the system. The main finding of our work is the successful control of the particles in the scattering region with a control smaller than noise. We have also analyzed and compared the escapes time of orbits in the scattering region for different situations. Finally, we believe that our results might contribute to a better understanding of both chaotic scattering phenomena and the application of the partial control technique to continuous dynamical systems.

Keywords: Controlling chaos; chaotic scattering; escaping dynamics.

1. Introduction

Open Hamiltonian dynamical systems have received much attention in the past few years in the context of transient chaos and chaotic scattering. The main reason resides in the fact that they are being used to model a wide range of phenomena in very different fields of physics. Some applications are the analysis of the escape of stars from galaxies [Contopoulos *et al.*, 1993; Contopoulos, 1990], the dynamics of ions in electromagnetic traps [Horvath *et al.*, 1998], the interaction between the Earths magnetotail and the solar wind [Chen *et al.*, 1990], and the study of geodesics in gravitational waves [Veselý & Podolský, 2000],

among others. All these applications are different manifestations of chaotic scattering, which basically consists of the interaction of a particle with a system that scatters it, in a way that the final conditions of speed and direction depend on the initial conditions in an extremely sensitive way (see [Bleher *et al.*, 1990] for a detailed study of this phenomenon). Typically for energies above a certain threshold value, which is commonly called the escape energy, the orbits are unbounded and several exits may appear in such a way that particles inside the scattering region leave it after a certain amount of time. However, if the energy is below this threshold value, there are no exits and consequently escapes are not possible. Chaotic scattering is normally associated with the dynamics of open Hamiltonian systems with chaotic properties. The possibility of an orbit to escape from the attraction of the corresponding potential is one of the main characteristics of this kind of systems. Usually, a particle bounces for a certain time in a bounded area called the scattering region, and eventually leaves it through one of the several exits, and it never comes back.

In this paper, we consider the conservative Hénon–Heiles Hamiltonian for energy values above the escape energy, so that the corresponding potential has exits; and trajectories starting at the interior of the potential are unbounded. Furthermore, we consider the situation in which there is noise, in such a way that it influences the escape of the trajectories from the scattering region. Since the pioneering work on controlling chaos, the OGY method [Ott *et al.*, 1990], different control schemes have been proposed that typically allows one to obtain a desired response from a dynamical system by applying some small but accurately chosen perturbations. In this context, some techniques that allow avoiding escapes in open dynamical systems presenting transient chaos have been proposed, with applications to many different fields in Physics and Engineering, see e.g. [Pyragas, 1992; Aguirre *et al.*, 2004]. The main goal of the paper is to use a control technique aiming at keeping trajectories inside the scattering region with a control intensity smaller than the environmental noise present in the system.

Keeping in mind that in most realistic situations, the trajectories of the particles can be affected by environmental noise [Mills, 2006], it will be an obstacle if escapes need to be avoided. In the presence of noise, we can imagine three different scenarios for control. If the control applied on the system's trajectories is larger than the amplitude of the noise, we should find quite easily a control strategy to keep the trajectories inside the scattering region. If the control applied is equal to the intensity of the noise, there are strategies that allow one to keep the trajectories inside the scattering region. But there is a third possibility: a control smaller than the amplitude of the noise. This is achieved by making use of the partial control technique recently described in [Zambrano *et al.*, 2008; Zambrano & Sanjuán, 2009]. This type of control does not tell where the trajectories will go exactly, it only drives the particle towards the closer point of a particular set. By doing so, escapes are avoided with a control smaller than the noise [Zambrano & Sanjuán, 2010]. Thus far, the partial control technique has been applied to discrete one-dimensional [Aguirre *et al.*, 2004], and two-dimensional systems, but never in a problem of chaotic scattering. In this paper, we show how to implement this control technique in a chaotic scattering problem described by the Hénon–Heiles system in presence of noise.

The organization of the paper is as follows. In Sec. 2, we sketch the main features of the partial control technique. Section 3.1 describes our model and the nature of the orbits. The analysis of the noise and its effect on the dynamics of the system is carried out in Sec. 3.2. Section 3.3 analyzes how the partial control technique can be applied to our system. Finally, some concluding remarks appear in Sec. 4.

2. The Partial Control Technique

We sketch here the basic ingredients of the partial control technique. We consider that the unperturbed dynamics of the system that we want to control is given by the one-to-one map $p_{n+1} = f(p_n)$. Moreover, we assume that there is a region in phase space Q from which nearly all trajectories escape under iterations of the map. The dynamics inside that region can be complex due to the presence of a zero-measure nonattractive chaotic set (i.e. a chaotic saddle). The aim of partial control is to avoid escapes from Q in the presence of noise with a control smaller than noise.

As in most physical applications, trajectories might be deviated due to the action of the environmental noise. This can be modeled in our equations as $p_{n+1} = f(p_n) + u_n$, where u_n is the noise and we assume it is bounded, $\|u_n\| \leq u_0$.

In order to keep trajectories bounded, we apply an accurate control r_n at each iteration, where we also assume it is bounded, $\|r_n\| \leq r_0$, by a positive constant r_0.

The global dynamics of our system is given by the equations

$$q_{n+1} = f(p_n) + u_n, \quad p_{n+1} = q_{n+1} + r_n, \quad (1)$$

where the control r_n depends on p_n and u_n.

Even if the trajectories typically escape from Q and the system is affected by noise of upper bound u_0, the partial control technique allows one to keep the trajectories bounded even if the upper bound control r_0 is smaller than the upper bound noise u_0, that is $\|r_0\| \leq u_0$. This is possible due to the existence of certain sets, which are called *safe sets* [Zambrano *et al.*, 2008; Zambrano & Sanjuán, 2009], inside the region Q. Initially, these safe sets were thought to be zero-measure sets inside Q, having the property that a particle may stay on them once the control is applied after having been pushed by a certain amount of noise. These safe sets were found to be curves for horseshoe maps [Zambrano *et al.*, 2008]. Later, it was shown that these safe sets could be "thicker" and related with the escape time sets, i.e. the set of points inside Q that escape from it under certain number of iterations [Sabuco *et al.*, 2010]. Recently an algorithm called Iterative Sculpting Algorithm [Sabuco *et al.*, 2011] has been designed by which the safe sets can be detected automatically by discarding points from a certain initial set within Q, without even needing to know exactly the system's equations.

3. Application of the Control Strategy to the Hénon–Heiles System

3.1. *The Hénon–Heiles system map*

The Hénon–Heiles Hamiltonian is a well-known model for an axisymmetrical galaxy [Hénon & Heiles, 1964], and it has been used as a paradigm in Hamiltonian nonlinear dynamics. It is a two-dimensional time-independent dynamical system and for values of the energy above the escape energy, its potential shows three different exits [see Fig. 1(a)]. The Hamiltonian equation is

$$H = \frac{1}{2}(\dot{x}^2 + \dot{y}^2) + \frac{1}{2}(x^2 + y^2) + x^2 y - \frac{1}{3}y^3, \quad (2)$$

(a)

(b)
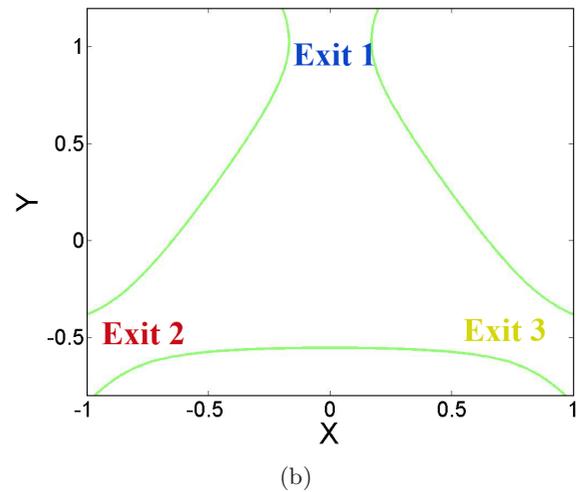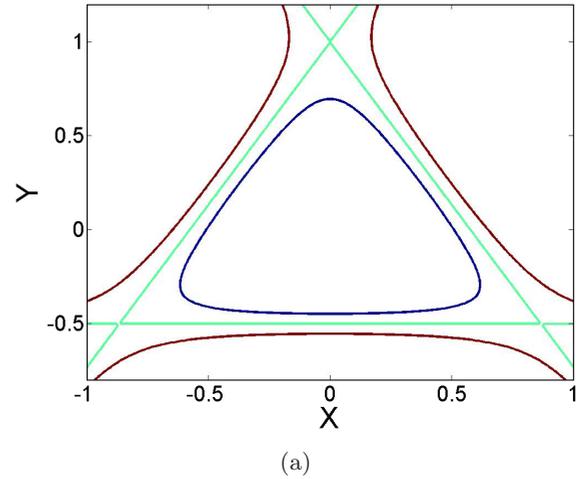
Fig. 1. (a) The isopotential curves of the Hénon–Heiles system for different values of the energy, in which both bounded and unbounded motions can take place. (b) Plots of the isopotential curves for $E = 0.21$.

and for $E_e = 1/6$, it shows an equipotential line that is an equilateral triangle. For energy values above the escape energy, the trajectories are unbounded and the system presents three exits, with a $2\pi/3$ rotation symmetry. At each exit there exists an unstable orbit, known as Lyapunov orbit, acting as frontiers. Any trajectory that crosses any one of them with an outward-oriented velocity goes to infinity and never comes back. We are interested in a situation with escapes from the scattering region, so from now on we fix the value of the energy to be $E = 0.21$, for which the system shows three exits as shown in Fig. 1(b).

The Hénon–Heiles Hamiltonian has a three-dimensional phase space, due to the conservation of the energy. In order to obtain a map associated with the dynamics of the system, we consider
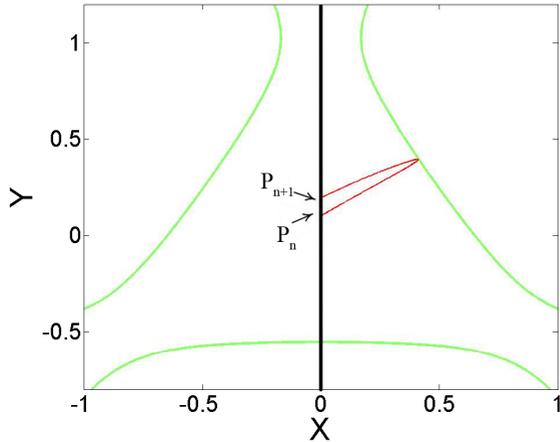
Fig. 2. The Poincaré map, there is a one-to-one relation between the nth intersection with $x = 0$ Poincaré surface, and the $(n + 1)$st, so $p_{n+1} = f(p_n)$. The coordinates of p_n are the y coordinate and the y component of the velocity, that is, $p_n = (y_n, \dot{y}_n)$.

the dynamics on an adequate Poincaré map. A convenient Poincaré map for the Hénon–Heiles system is obtained with the intersection of the trajectories with the surface of section $x = 0$. The map, defined as

$$
\begin{aligned}
p_{n+1} &= f(p_n) \\
p_n &= (y_n, \dot{y}_n),
\end{aligned}
\tag{3}
$$

is a one-to-one relation between p_n and p_{n+1} as shown in Fig. 2, where y and $\dot{y}$ are the y coordinate and the velocity projection on the y axis for the

nth intersection of the trajectory with the surface section $x = 0$.

Every initial condition starting inside the scattering region escapes through any of the exits described above, therefore, in this case we cannot talk about attractors. However, we can define exit basins in an analogous way to the basins of attraction in a dissipative system. A basin of attraction is the set of initial conditions in phase space that are attracted to a specific attractor. Analogously, an exit basin is the set of initial conditions in phase space leading to a certain exit. In order to see this, we can draw the exit basin [Aguirre *et al.*, 2001] of the system by assigning a different color to each initial point $p = (y, \dot{y})$ depending on the exit through which it leaves the scattering region.

The exit basin is shown in Fig. 3(a), where we can see that all trajectories leave the scattering region. The time the particle spends to leave the potential well, the escape time, depends on the initial condition of the system. In the context of our problem, we can measure two kinds of escape times. The first one is the continuous time, that is, the real time the particle spends inside the scattering region. The second one is the discrete time, that is, the number of intersections of the Poincaré surface on any trajectory starting from it before escaping. In order to have a deeper insight on the system's dynamics, as well as a necessary preliminary step in order to determine the safe sets

(a)

(b)
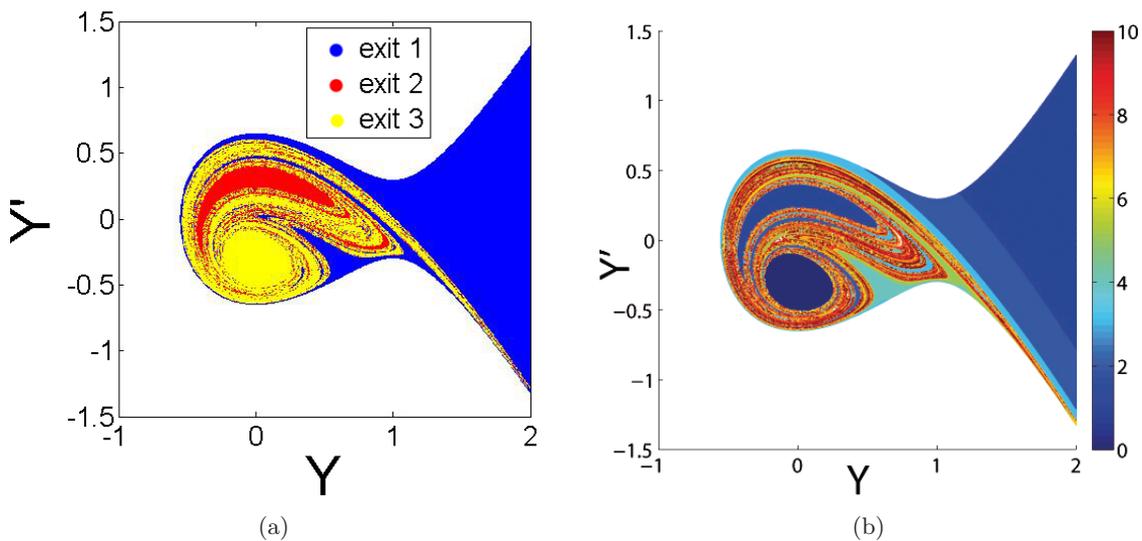
Fig. 3. (a) The exit basins, so each color denotes the exit through which trajectories with that initial condition escape: exit 1 (blue, $(y \to +\infty)$), exit two (red, $(y \to -\infty, x \to -\infty)$) and exit 3, (yellow $(y \to -\infty, x \to +\infty)$). (b) The escape times, the colored gradient from blue to red indicates the growth of the escape times. Both figures are painted in the Poincaré section $(y, \dot{y})$, without noise.
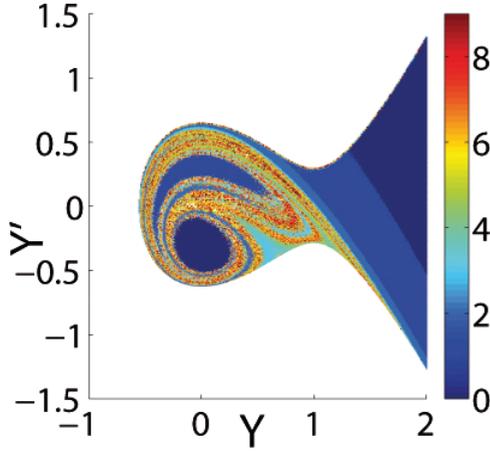
Fig. 4. The figure shows the escape time sets computed for $D = 10^{-5}$, as in Fig. 3, the colored gradient from blue to red indicates the growth of the escape times. It is painted in the Poincaré section $(y, \dot{y})$.

[Sabuco *et al.*, 2011], we have computed the discrete escape times for points in the Poincaré surface in Figs. 3(b) and 4, respectively with and without noise, in which the color bar denotes the discrete escape time of every initial condition. We can see that all points in this figure have finite escape times. Furthermore, as expected, we can see by looking at Figs. 3(a) and 3(b) that the higher escape times correspond to points close to the boundary between the three exit basins.

3.2. *The continuous and the discrete noise*

In the context of our chaotic scattering system, noise is introduced in a natural way as follows [Seoane & Sanjuán, 2008; Seoane *et al.*, 2009]:

$$\ddot{x} + x + 2xy = D\xi(t)$$
$$\ddot{y} + y + x^2 - y^2 = D\eta(t), \tag{4}$$

where $\xi(t)$ and $\eta(t)$ are unit Gaussian random processes and D is the noise intensity. Note that $D = 2\sigma^2$, where σ is the standard deviation of the noise acting on our system. The introduction of noise can change the dynamics of the system in a drastic way [Seoane *et al.*, 2009]. For example, we can see in Figs. 5(a) and 5(b) respectively, how the trajectory of a particle starting from the same initial condition changes. In fact, we can calculate the exit basins for the system in the presence of noise, and we can see how its structure drastically changes, becoming blurred, as observed in Fig. 6.

(a)

(b)
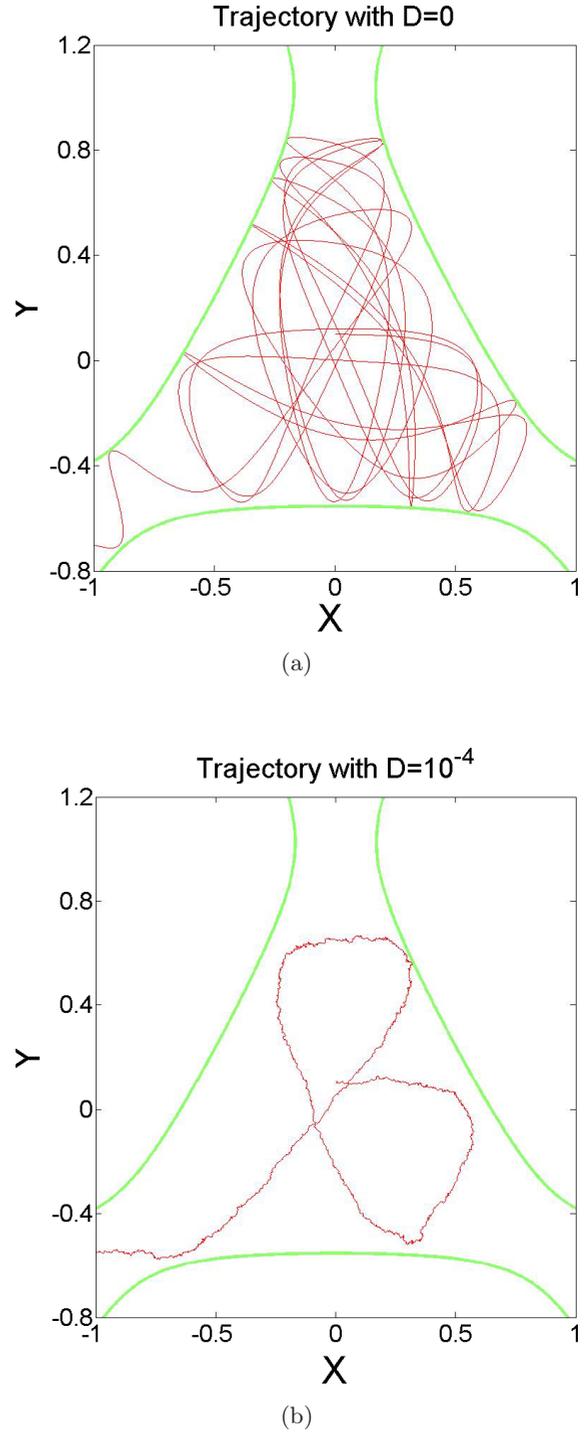
Fig. 5. (a) A typical trajectory of a particle, without noise inside the Hénon–Heiles potential we used. The continuous escape time for this trajectory is 93, while the discrete escape time is 27, namely the trajectory crosses the Poincaré section 27 times. (b) A typical trajectory affected by the noise, $D = 10^{-4}$. The continuous escape time for this trajectory is 14, while the discrete escape time is 3, namely the trajectory crosses the Poincaré section three times. In both pictures, the particle starts its trajectory inside the scattering region, at the initial point $(x_0, y_0) = (0, 0.1)$ with an angle $\theta = \pi/2$ and leaves it after some bounces against the potential walls.
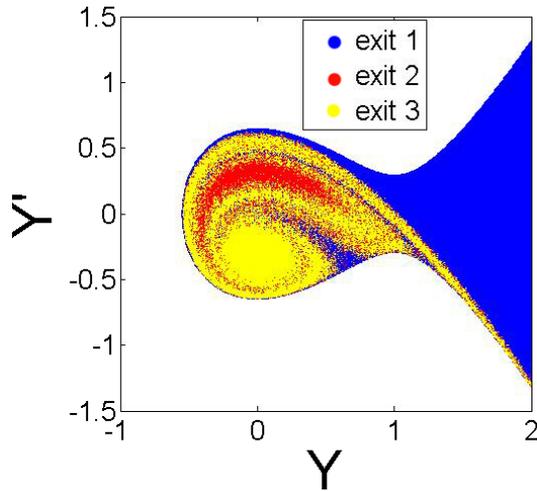
Fig. 6. This figure shows the same set as of Fig. 5(a) with a noise intensity $D = 10^{-5}$. The figure is painted in the Poincaré section $(y, \dot{y})$.

In order to investigate the relation between the noise intensity D and the escape times, we plot Fig. 7, that shows the average discrete escape time T_d versus the noise intensity D. This picture has been built by computing the mean of 100 realizations for every value of D. We can observe, for very low values of noise, an increase of the discrete time escape T_d. This is in agreement with the results shown in [Altman & Endler, 2010] but for a continuous-time system instead of a map. The preservation, for very low amount of noise, of structures like the KAM islands is responsible for larger escape times compared to the noiseless case. On the other hand, when the system is completely noisy these structures are destroyed and the phase space
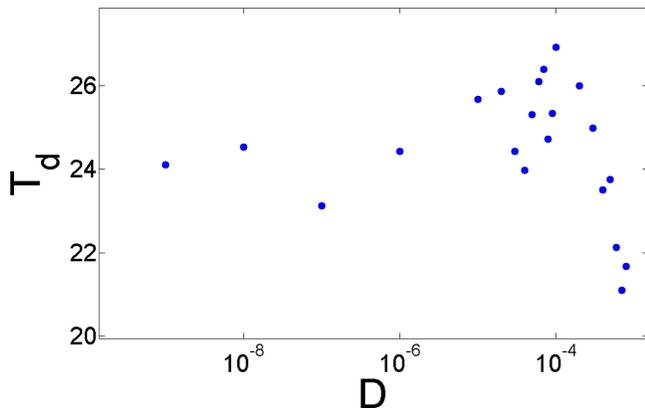
Fig. 7. This figure shows the relation between the noise intensity, D, and the discrete escape time. The diagram shows a sudden variation after the value $D = 10^{-4}$, when finally time starts to decrease for higher values of noise.

appears to be smeared. This results in the particles escaping very fast from the scattering region and it explains the decreasing of T_d only after the value $D = 10^{-4}$, as shown in Fig. 7.

In order to apply the partial control technique, we need to distinguish between two kinds of noise.
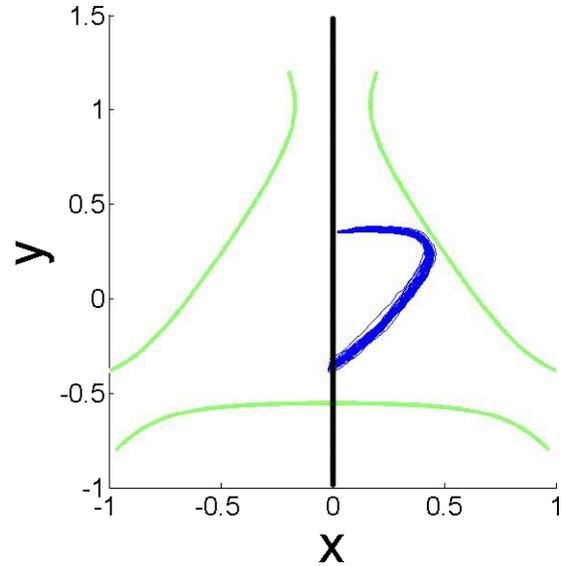
(a)
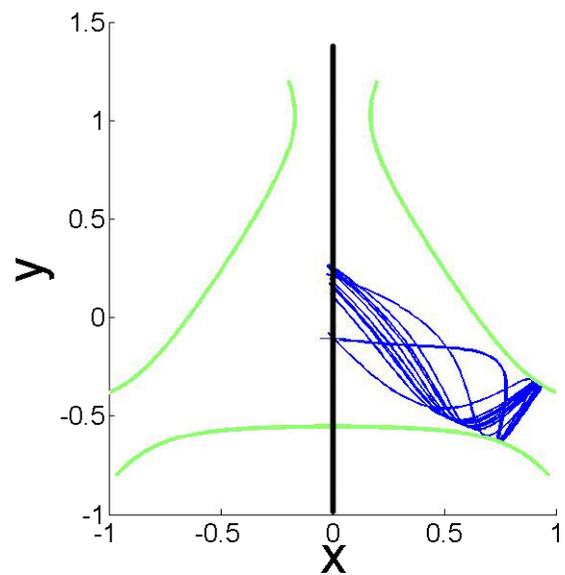
(b)

Fig. 8. (a) The dispersion on the Poincaré surface of the first iteration of 50 trajectories, with the same initial conditions, $(x_0, y_0) = (0, 0.4), \theta = \pi/2$, and affected by continuous noise. (b) 50 trajectories with a big dispersion on the Poincaré map. In (a) the bunch of trajectories is much more coherent, while in (b) it is diffused on the axis $x = 0$. The two bunches of trajectories are calculated with the noise $D = 10^{-6}$.
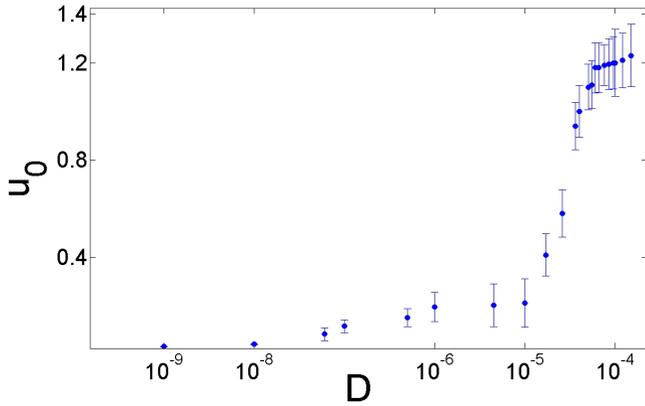
Fig. 9. This figure shows the relation between the intensity of the noise D and u_0. The diagram shows a sudden variation after the value $D = 10^{-5}$.

The first one is that mentioned above, which affects directly and continuously the trajectory as shown in Fig. 5(b). We call it *continuous* noise. We see trajectories starting with the same initial condition on the Poincaré section with different noise realizations in Figs. 8(a) and 8(b). We observe that the iteration of a given point p_n on the Poincaré section is not $f(p_n)$, due to the presence of noise. The effect of the continuous noise on the dynamics of the Poincaré map is what we call the *discrete* noise. Formally, under the noisy Poincaré map we have $f(p_n) + u_n$, where u_n such that $|u_n| \leq u_0$,
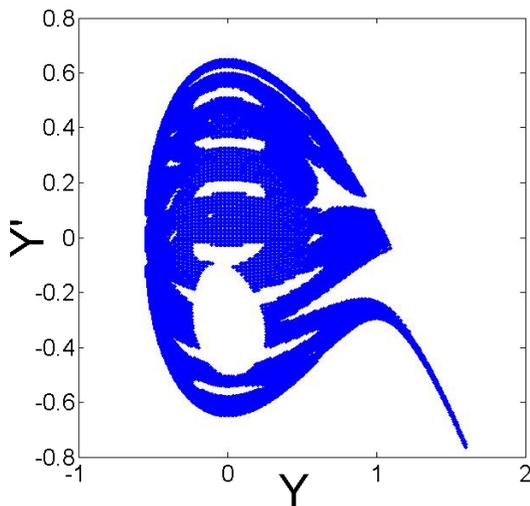
Fig. 10. The safe set computed using our algorithm for $D = 10^{-7}$. After discarding the points with escape time equal to zero, and the points with a high sensitivity to noise, an algorithm is applied to calculate the safe set, where trajectories are kept inside the scattering region with a control smaller than noise.
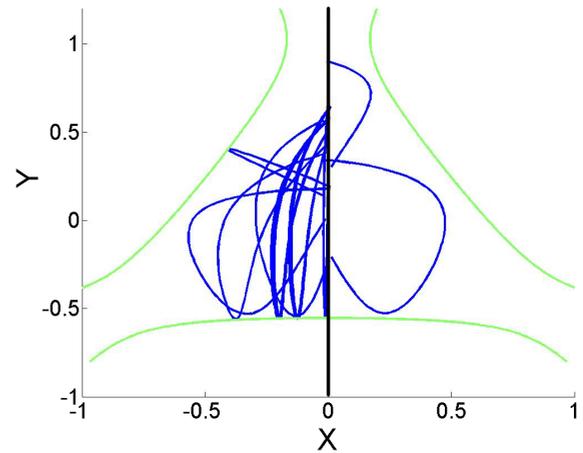
(a)
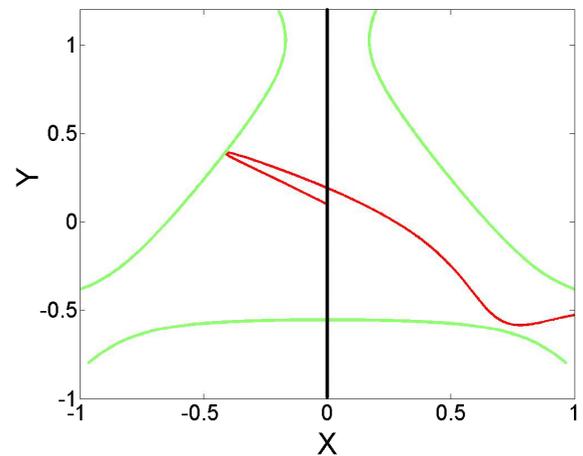
(b)

Fig. 11. (a) An example of a controlled trajectory in the (x, y) plane. (b) The same trajectory without the control. The value of the noise intensity that we have used is $D = 10^{-7}$ and the initial conditions are $(x_0, y_0) = (0, 0.1)$, and $\theta = 1.7$. For the controlled trajectory we show only 12 iterations for clarity.

is our discrete noise. Now we need to characterize the relation existing between the upper bound of the discrete noise u_0 and D. To estimate this relation, we compute a sufficiently large ensemble of orbits starting from different initial points p_n on our Poincaré section. After one iteration, each one of them will intersect again the Poincaré section at a new point $p'_{n+1} = f(p_n) + u_n$. We consider the difference between p'_{n+1} and the expected value in the absence of noise, $f(p_n)$, a measurement of the discrete noise. The upper bound u_0 of the discrete noise is the maximum value obtained. The process, though, presents some complications that need to
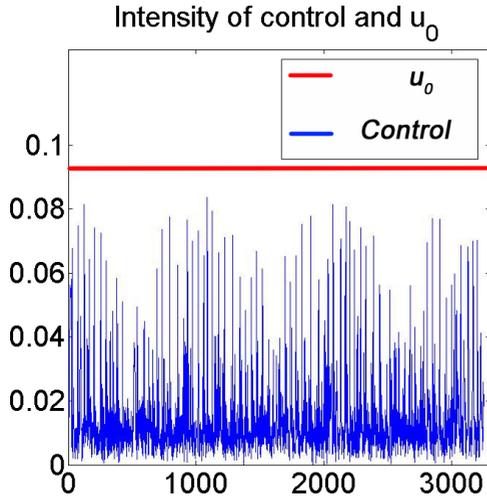
Fig. 12.   The figure shows the control applied at each iteration and we can observe that this control is always smaller than the noise u_0.

(a)

(b)

Fig. 13.   (a) The discrete escape time of some controlled trajectories, with a control $r_0 < u_0$, related to the angles, $(0 - 2\pi)$ with a noise $D = 10^{-7}$. (b) The number of iterations for the same ensemble of trajectories of (a) but without control.

be overcome. In particular, we find that some points p_n do not come back to the Poincaré section when the noise is present, so we discard them because they are not useful to later compute the safe sets [Sabuco *et al.*, 2011]. Moreover, we find that the sensitivity to noise of some initial points p_n is very high. In particular, our numerical simulations show that the value of the discrete noise for certain points is abnormally high. This can be seen clearly in Fig. 8. For a fixed value of noise intensity $D = 10^{-6}$, we see that for certain trajectories, as shown in Fig. 8(b), the discrete noise is much higher, as compared with the trajectories shown in Fig. 8(a). These points with high sensitivity to noise are crucial for the application of the partial control technique and, in particular, for any control technique involving the use of an adequate Poincaré map.

For moderate noise values, there are not so many points with high sensitivity to noise. Thus, in order to get rid of them, one can compute the discrete noise for each point in the Poincaré section and discard a small fraction, for example, points with the top 2% values. The value of u_0 will then be the maximum value of the discrete noise of the remaining 98% of the considered points. And these simulations have been done for different values of the noise intensity D. The results are shown in Fig. 9. We can observe that the value of u_0 increases until reaching a plateau for $D \approx 10^{-4}$. Note that when the noise intensity D is higher than 10^{-5}, there is a strong increase of the upper bound of the discrete noise u_0. This is related to the destruction

of KAM islands in phase space [Altman & Endler, 2010]. These effects on the topology of the system increase the importance of the noise effect on the Poincaré map, so we think that this plateau is due to the fact that discarding only 2% of the points is insufficient to get rid of all the points with high sensitivity to noise.

3.3. *The application of the partial control technique*

After having discarded these points mentioned before, we use the remaining points to compute the safe set by applying the algorithm described in [Sabuco *et al.*, 2011]. We plot these safe sets for a noise intensity $D = 10^{-7}$ in Fig. 10. An example of application of the partial control technique with this safe set is shown in Fig. 11(a), whereas in Fig. 11(b) we can see how the trajectory suddenly escapes
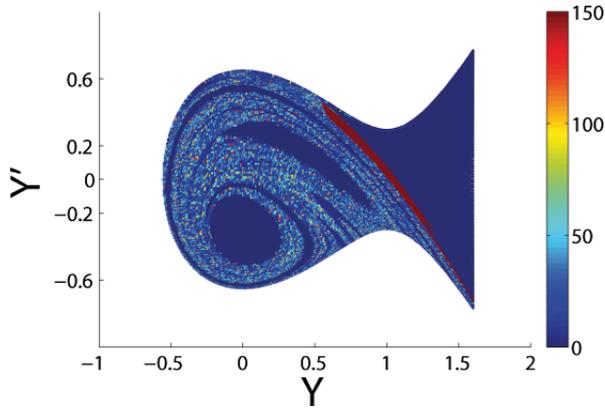
Fig. 14. The figure shows the discrete escape time of every initial condition as in Fig. 3(b), but with the control $r_0 < u_0$ applied. The gradient bar shows the escape time from the minimum 0, in blue, to a maximum, 100, in dark red. Note that the escape times are longer as compared to the noisy and the deterministic cases, Figs. 4 and 3(b) respectively.

from the scattering region in the absence of control. The control needed to keep the trajectories bounded is shown in Fig. 12: we can see that the necessary control applied is smaller than the value of the estimated discrete noise u_0. In other words, there is a control r_0 such that trajectories can be kept inside the scattering region by applying a control smaller than noise, $r_0 < u_0$.

For trajectories starting on the safe set, the escape time would be infinite, provided that any trajectory starting on it can be kept bounded forever with a control $r_0 < u_0$. However, it is interesting to see how the escape time sets of the remaining points in the Poincaré section are affected. This is shown in Fig. 13(a). We observe that controlled trajectories have escape times always larger than those uncontrolled, as shown in Fig. 13(b).

Furthermore, it is possible to see the effect of applying this control to all points in the scattering region. This is shown in Fig. 14, where it is possible to see how the escape times are larger than in the noisy chaotic scattering, Fig. 4, and in the deterministic chaotic scattering, Fig. 3(b). In this picture, in fact, it is possible to see that the colored gradient scale can reach the escape time value of 100, while in the other two cases this same gradient scale does not overcome the value of 10. In short, we have been able to keep trajectories inside the scattering region by applying a control smaller than the noise $r_0 < u_0$, once a convenient Poincaré map is chosen, and the discrete noise and the safe sets are computed.

4. Conclusions

We have shown in this work how to apply the partial control technique to a noisy chaotic scattering problem. The application of the technique relies on an appropriate choice of a Poincaré map and on the estimation of the effect of noise. In doing so, we have noticed the existence of certain points of high sensitivity to noise, which are points whose trajectories are greatly affected by noise. After discarding these points and those that escape without intersecting again the Poincaré section, one can estimate the value of the discrete noise u_0 and use the Iterative Sculpting Algorithm to determine the safe sets. After this, the partial control technique is successfully applied for the first time for a continuous-time dynamical system in the presence of noise. We have also analyzed and compared the escape times of orbits starting in the scattering region for different situations, either in the absence of noise or in the presence of noise or when the control is applied in the presence of noise. We believe that the ideas described in this work might contribute to the applicability of the partial control technique to a wider variety of problems.

Acknowledgment

References

Aguirre, J., d'Ovidio, F. & Sanjuán, M. A. F. [2004] "Controlling chaotic transients: Yorke's game of survival," *Phys. Rev. E* **69**, 016203.

Aguirre, J., Vallejo, J. C. & Sanjuán, M. A. F. [2001] "Wada basin and chaotic invariant sets in the Hénon–Heiles system," *Phys. Rev. E* **64**, 066208.

Altmann, E. G. & Endler, A. [2010] "Noise-enhanced trapping in chaotic scattering," *Phys. Rev. Lett.* **105**, 244102.

Bleher, S., Grebogi, C. & Ott, E. [1990] "Bifurcation to chaotic scattering," *Physica D* **46**, 87–121.

Chen, J., Rexford, J. L. & Lee, Y. C. [1990] "Fractal boundaries in magnetotail particle dynamics," *Geophys. Res. Lett.* **17**, 1049–1052.

Contopoulos, G. [1990] "Asymptotic curves and escapes in Hamiltonian systems," *Astron. Atrophys.* **231**, 41–55.

Contopoulos, G., Kandrup, H. E. & Kaufman, D. [1993] "Fractal properties of escape from a two-dimensional potential," *Physica D* **64**, 310–323.

Hénon, M. & Heiles, C. [1964] "The applicability of the third integral of motion: Some numerical experiments," *Astron. J.* **69**, 73–79.

Horvath, G. Z. K., Hernández Pozos, J. L., Dholakia, K., Rink, J., Segal, D. M. & Thompson, R. C. [1998] "Ion dynamics in perturbed quadrupole ion traps," *Phys. Rev. A* **57**, 1944–1956.

Mills, P. [2006] "The influence of noise on a classical chaotic scatterer," *Commun. Nonlin. Sci. Numer. Simul.* **11**, 899–906.

Ott, E., Grebogi, C. & Yorke, J. A. [1990] "Controlling chaos," *Phys. Rev. Lett.* **64**, 1196–1199.

Pyragas, K. [1992] "Continuous control of chaos by self-controlling feedback," *Phys. Lett. A* **170**, 421–428.

Sabuco, J., Zambrano, S. & Sanjuán, M. A. F. [2010] "Partial control of chaotic transients and escape times," *New J. Phys.* **12**, 113038.

Sabuco, J., Zambrano, S. & Sanjuán, M. A. F. [2011] "Iterative sculpting algorithm: A general algorithm to compute safe sets for partial control of chaotic systems," *Commun. Nonlin. Sci. Numer. Simul.*

Seoane, J. M., Huang, L., Sanjuán, M. A. F. & Lai, Y. C. [2009] "Effect of noise on chaotic scattering," *Phys. Rev. E* **79**, 047202.

Seoane, J. M. & Sanjuán, M. A. F. [2008] "Exponential decay and scaling laws in noisy chaotic scattering," *Phys. Lett. A* **372**, 110–116.

Veselý, K. & Podolský, J. [2000] "Chaos in a modified Hénon–Heiles system describing geodesics in gravitational waves," *Phys. Lett. A* **271**, 368–376.

Zambrano, S., Sanjuán, M. A. F. & Yorke, J. A. [2008] "Partial control of chaotic systems," *Phys. Rev. E* **77**, 055201(R).

Zambrano, S. & Sanjuán, M. A. F. [2009] "Exploring partial control of chaotic systems," *Phys. Rev. E* **79**, 026217.

Zambrano, S. & Sanjuán, M. A. F. [2010] "Partial control of chaotic systems," *Recent Progress in Controlling Chaos*, eds. Sanjuán, M. A. F. & Grebogi, C. (World Scientific, Singapore), pp. 315–336.